

Simulating the Giant Magnetocaloric Effect - from Mean-Field Theory to Microscopic Models

J. S. Amaral¹, V. S. Amaral^{1,*}

¹ Departamento de Física and CICECO - Aveiro Institute of Materials, University of Aveiro, Portugal

Correspondence*:

Vítor Amaral, Departamento de Física, Universidade de Aveiro, 3810-193 Aveiro, Portugal
vsamaral@ua.pt

2 ABSTRACT

Magnetocaloric materials are recognized as one of the major classes of magnetic materials for energy applications, and can be either employed as refrigerants in heat-pumping devices, or in thermomagnetic generators for energy conversion/harvesting. For both applications, having a material that presents a first-order magnetic phase transition is advantageous, as this typically leads to enhanced values of magnetization change in temperature (relevant to energy conversion) and of the magnetocaloric effect (relevant to heat-pumping). We present a brief overview of selected models applied to the simulation of applied magnetic field and temperature-dependent magnetization and magnetic entropy change of first-order magnetic phase transition systems, covering mean-field models such as the Landau theory of phase transitions and the Bean-Rodbell model, up to more recent developments using a Ising-like microscopic model with magnetovolume coupling effects. We highlight the fundamental and practical limitations of employing these models and compare predicted thermodynamic properties.

Keywords: Magnetic Materials, Magnetic Refrigeration, Energy Harvesting, First-order Phase Transitions, Magnetovolume coupling

1 INTRODUCTION

Magnetic materials have had, for several decades, wide-spread use in energy applications, including power generation, conditioning, conversion and transportation (Gutfleisch et al., 2011). Since the discovery of the giant magnetocaloric effect (GMCE) in the late 1990's (Pecharsky and Gschneidner Jr., 1997), the use of magnetic materials for room-temperature refrigeration has been gathering the attention from both the scientific and industrial communities (Pecharsky and Gschneidner Jr., 2008). The GMCE is typically observed only for first-order magnetic phase transition (FOMPT) materials, where a strong magnetovolume coupling is present. As the designation implies, the GMCE is considerably larger than the MCE of second-order magnetic phase transition (SOMPT) systems. While technologically challenging, the development and use of FOMPT materials for use in refrigeration devices is now commonplace, as seen from the number of current prototypes using these materials as refrigerants (Kitanovski et al., 2015). More recently, the use of magnetocaloric materials for energy generation from near room temperature thermal energy harvesting has also gathered attention (Waske et al., 2019). In this case, the sharp dependence of magnetization (M) on temperature (T) near the Curie temperature T_C of a FOMPT material enhances the energy-harvesting potential of a device, in a tunable operating temperature window. In short, for both refrigeration and

30 thermal energy harvesting, the use of a first-order magnetic phase transition (FOMPT) material presents
 31 considerable advantages. The search for new and optimized magnetocaloric materials for these applications
 32 is an on-going effort from the community. In this context, the use of magnetism models to both interpret
 33 experimental data and predict the magnetic and magnetocaloric performance of materials are valuable
 34 tools. Naturally, correctly describing the thermodynamics of a FOMPT is required to ensure the physical
 35 soundness of calculations. Nevertheless, when choosing a model to use, practical questions come into play,
 36 and in the end, the choice of a particular model becomes the result of the balance between the complexity
 37 of the model, the information being sought, and the computational cost.

38 In this work, we consider three distinct models which have been employed to describe quantitatively
 39 describe FOMPT materials, from mean-field models such as the Landau theory of phase transitions, the
 40 Bean-Rodbell model, and a microscopic Ising-like model with magnetovolume interactions. We employ
 41 these models to simulate both SOMPT and FOMPT systems with similar thermodynamic properties, such
 42 as a $T_C \sim 300$ K for the SOMPT, same spin values and saturation magnetization, and a similar value of
 43 critical field for the FOMPT system. Both magnetic field (H) and T dependent M and magnetic entropy
 44 change (ΔS_M) are simulated for the three considered models. The aim is to compare the obtained results
 45 both qualitatively and quantitatively, highlighting the fundamental and practical limitations of employing
 46 these models to describe real materials.

2 THE LANDAU THEORY OF PHASE TRANSITIONS

47 The Landau theory of phase transitions has been previously employed to describe the GMCE of FOMPT
 48 systems, from describing the magnetoelastic coupling influence on the magnetocaloric effect in ferromag-
 49 netic materials (Amaral and Amaral, 2004), and the effect of magnetic irreversibility on estimating the
 50 magnetocaloric effect from magnetization measurements (Amaral and Amaral, 2009). The model starts
 51 from an expansion of the (Gibbs) Free Energy G on even powers of M , together with an Zeeman-like
 52 external field interaction term.

$$G(T, M) = G_0 + \frac{1}{2}A(T)M^2 + \frac{1}{4}B(T)M^4 + \frac{1}{6}C(T)M^6 - M.H, \quad (1)$$

53 where A , B , and C are the temperature-dependent Landau coefficients. Typically A is assumed to be linear
 54 in temperature, establishing the Curie temperature T_C of the system: $A(T) = A'(T - T_C)$. This linear
 55 relation is valid in the susceptibility regime, obeying the Curie law:

$$\frac{H}{M} = \frac{C_{Curie}}{T - T_C}, \quad (2)$$

56 where C_{Curie} is the Curie constant of the system. For low M values, the A' parameter is then equal to the
 57 inverse Curie constant. Minimizing the free energy expression of equation 1, an equation of state is derived:

$$\frac{H}{M} = A(T) + B(T)M^2 + C(T)M^4, \quad (3)$$

58 with a structure that allows fitting the well-known isothermal Arrott plot (H/M versus M^2) construction
 59 to determine the Landau coefficients' dependence on temperature from magnetization data. This approach
 60 was employed for both FOMPT (Amaral and Amaral, 2004) and SOMPT (Amaral et al., 2005) systems.

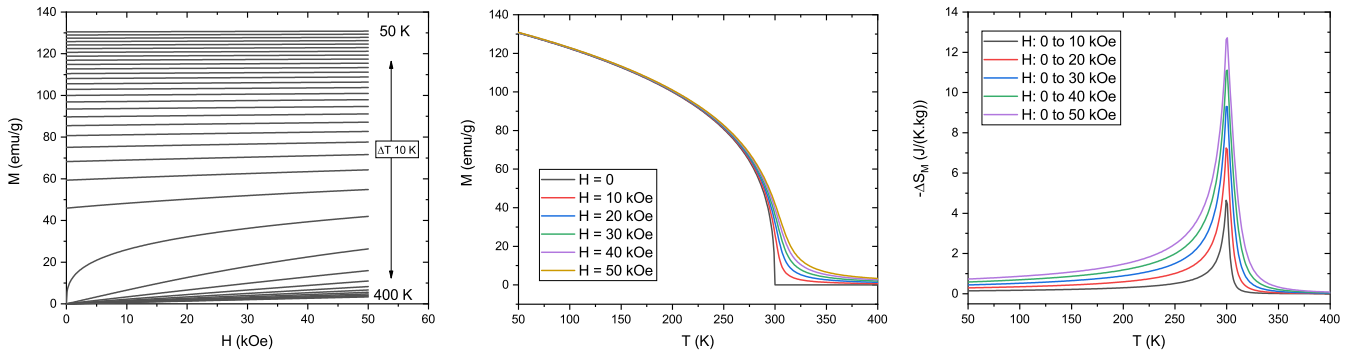


Figure 1. (A) Isothermal magnetization M versus applied magnetic field H , of a SOMPT system simulated by the Landau theory of phase transitions. Simulation parameters where chosen to correspond to a magnetic material with spin 1/2 and a saturation magnetization value of 100 emu/g. (B) Isofield M versus temperature T behavior, for H between 0 and 50 kOe. (C) Magnetic entropy change ΔS_M dependence on H change and T .

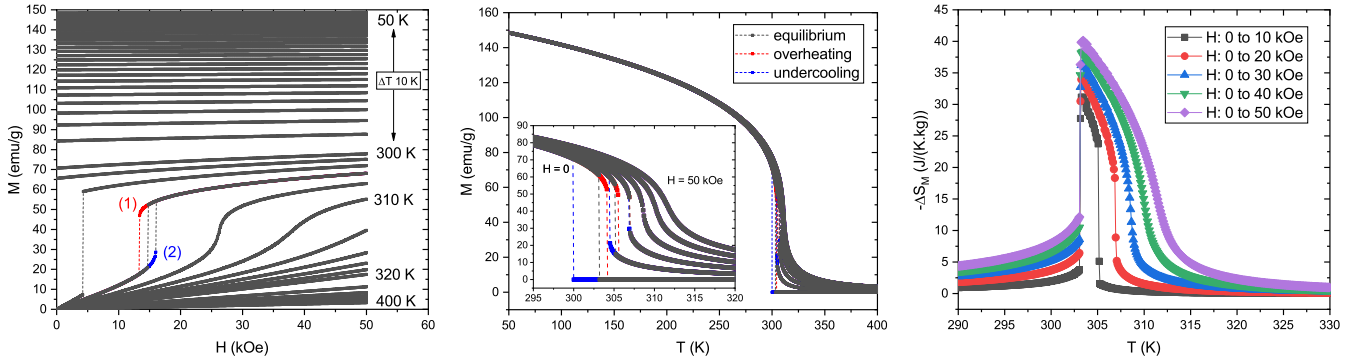


Figure 2. (A) Isothermal magnetization M versus applied magnetic field H , of a FOMPT system simulated by the Landau theory of phase transitions. Simulation parameters where chosen to correspond to a magnetic material with spin 1/2 and a saturation magnetization value of 100 emu/g, with a critical field value ~ 25 kOe. (B) Isofield M versus temperature T behavior, for H between 0 and 50 kOe. (C) Magnetic entropy change ΔS_M dependence on H change and T .

61 Here, we consider a trial system with $A' = 1.5 \times 10^2$, and constant B and C coefficients, $\pm 5 \times 10^{-1}$ and
 62 1×10^{-4} respectively in cgs units, with $T_C = 300$ K. The A' value was chosen to correspond to the inverse
 63 Curie constant of a molecular mean-field system with spin $S = 1/2$, and a saturation magnetization of 100
 64 emu/g. The chosen B value leads, when negative, to a critical field of ~ 25 kOe which is within values
 65 achievable in commercially available magnetometers with superconducting coils as applied field source.

66 The $M(H, T)$ and $\Delta S_M(H, T)$ data of Figure 1, using a positive B coefficient, show how a system with
 67 thermomagnetic behavior comparable to real SOMPT systems is obtained, with M around 40 emu/g at 50
 68 kOe near T_C , and a maximum value of ΔS_M around 12 J/(K·kg) for a field change from 0 to 50 kOe.

69 When considering a negative B coefficient value, the system now shows a FOMPT, where discontinuities
 70 are present in both the magnetization and magnetic entropy change dependence in T and H , as shown in
 71 Figure 2.

As expected, the maximum ΔS_M increases considerably, up to values $\sim 40 \text{ J/(K}\cdot\text{kg)}$. The FOMPT nature is clearly visible in the discontinuities in both $M(H, T)$ and $\Delta S_M(H, T)$ data. One of the main limitations of the Landau theory of phase transitions, in this context, is visible when the system reaches higher values of M . Due to the equation of state originating from a power expansion in M , the validity of this expansion fails for high M values, and the magnetization does not saturate even at very low T . This is an important fact that is often overlooked when fitting or extrapolating Arrott plots of experimental data in the high-magnetization regime. There is also no deep physical insight from the values of the B and C Landau parameters. One can observe a negative B value and justify its occurrence with effects such as magnetovolume coupling and electron condensation, depending on the particular physics of the system under study, but a quantitative analysis is typically not the objective of employing this model. As we will see in the next section, the use of the Bean-Rodbell model, overcomes some of these limitations.

3 THE BEAN-RODBELL MODEL

The Bean-Rodbell model is an extension to the Weiss molecular field model, and was first reported in a study on the magnetic properties of MnAs, a system well-known to have strong magneto-volume coupling (Bean and Rodbell, 1962). The model imposes a linear relation between T_C and volume, as shown in Equation 4.

$$T_C = T_0 \left(1 + \beta \left(\frac{v - v_0}{v_0} \right) \right), \quad (4)$$

where β is positive and constant, v is volume, v_0 the equilibrium volume with no magnetic interactions, and T_0 the Curie temperature of the rigid system with $v = v_0$.

For a sufficiently large linear dependence of T_C on volume (large β value), the magnetic transition becomes first-order. The crossover point is established via the η parameter, which is defined for a system with compressibility K :

$$\eta = 40Nk_BKT_0\beta^2 \frac{(S(S+1))^2}{(2S+1)^4 - 1}, \quad (5)$$

where S is the spin quantum number, N the spin density and k_B the Boltzmann constant. The transition is second-order for $0 < \eta \leq 1$, while for $\eta > 1$ the transition is first-order.

For a comparable system with the previous simulations using the Landau theory of phase transitions, we consider the following parameters for our Bean-Rodbell model calculations: $S = 1/2$, $T_0 = 300 \text{ K}$, and a N value of $1.077 \times 10^{22} \text{ spins/g}$, which corresponds to a saturation magnetization of 100 emu/g . For simulating a SOMPT, a null η value is used, with data for magnetization and magnetic entropy change shown in Figure 3.

For simulating a FOMPT, an η value of 1.35 is used, which increases the T_C to around 304 K, and leads to a critical field around 2.5 kOe, together with an increase in magnetic entropy change, as shown in Figure 4.

The Bean-Rodbell model simulation results are quite similar to those obtained by the Landau theory of phase transitions, for both the SOMPT and FOMPT. This could only be achieved by establishing comparable systems with the same Curie constant, and adjusting the values of the Landau B and the Bean-Rodbell η parameters to lead to similar values of the critical field. Note, however, how for the

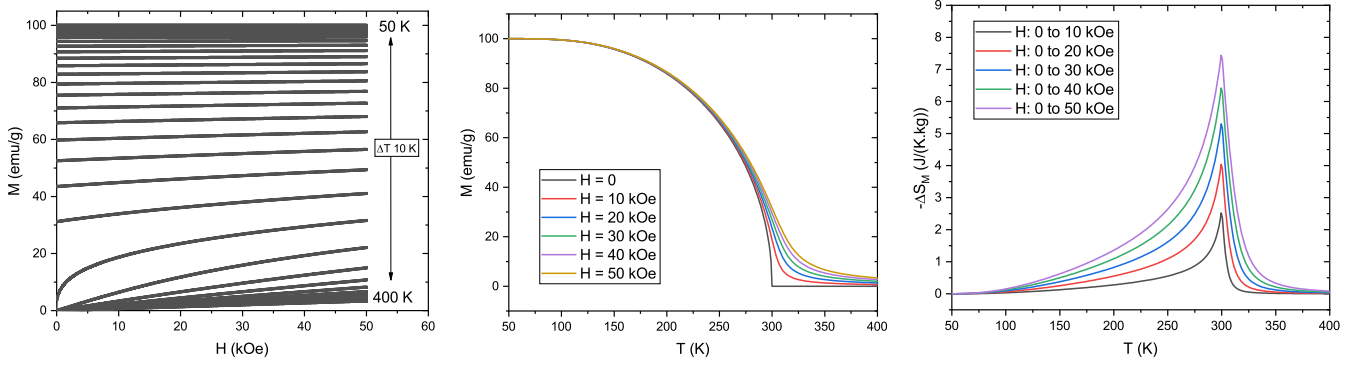


Figure 3. (A) Isothermal magnetization M versus applied magnetic field H , of a SOMPT system ($\eta = 0$) simulated by the Bean-Rodbell model, with spin 1/2 and a saturation magnetization value of 100 emu/g. (B) Isofield M versus temperature T behavior, for H between 0 and 50 kOe. (C) Magnetic entropy change ΔS_M dependence on H change and T .

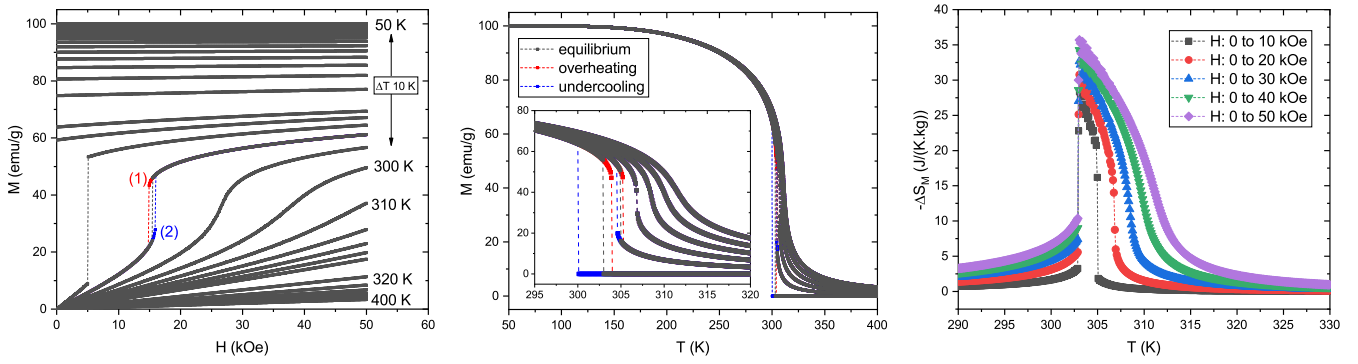


Figure 4. (A) Isothermal magnetization M versus applied magnetic field H , of a FOMPT system ($\eta = 1.35$) simulated by the Bean-Rodbell model, with spin 1/2 and a saturation magnetization value of 100 emu/g. (B) Isofield M versus temperature T behavior, for H between 0 and 50 kOe. (C) Magnetic entropy change ΔS_M dependence on H change and T .

106 Bean-Rodbell data, the $M(H, T)$ data clearly saturates. The use of the model in the high- M region was
 107 useful in the simulation of mixed-phase FOMPT materials, and the validity of the use of the Maxwell
 108 relation in estimating ΔS_M in strongly first-order systems (Amaral and Amaral, 2009, 2010). It is also
 109 worth highlighting that, as opposed to the Landau theory of phase transitions, the fact that physically
 110 meaningful parameters such as spin and compressibility are defined in the model, a quantitative analysis
 111 of experimental data using the Bean-Rodbell model is possible, for both FOMPT and SOMPT systems
 112 (Amaral et al., 2007). Simulations using this model are computationally inexpensive, and it is possible
 113 to consider smooth distributions of T_C values, with hundreds of points, to describe disordered SOMPT
 114 (Amaral et al., 2008; Bahl et al., 2012) and FOMPT (Amaral and Amaral, 2014; Nielsen et al., 2017)
 115 systems.

116 While widely employed in the study of both SOMPT and FOMPT materials, the Bean-Rodbell model is
 117 not the right model for predicting a given material's magnetic and magnetocaloric performance. For this,
 118 an ab-initio approach is required, which can start from using Density Functional Theory (DFT) to estimate
 119 relevant magnetic and physical properties of a given system. DFT calculations are typically performed at 0

120 K, so it is required to feed this parameters to a given model for estimating thermodynamic properties. A
 121 relatively straightforward approach is to estimate the Heisenberg exchange parameter J of a given material
 122 using DFT, and then use the calculated value in an Ising or Heisenberg model. Naturally, for describing a
 123 magneto-volume driven FOMPT, the model needs to include this coupling. In the next section, we will
 124 consider an Ising-like microscopic model with magnetovolume interactions.

4 MICROSCOPIC MODEL WITH MAGNETOVOLUME INTERACTIONS

125 A FOMPT system can be described in simple microscopic models, such as the Ising and Heisenberg models,
 126 by including an explicit dependence of the magnetic exchange parameter J , together with a volume energy
 127 potential (Amaral et al., 2016):

$$\mathcal{H} = -\frac{1}{2} \sum_{i,j} [J(v) S_i \cdot S_j] + \frac{1}{2} Kv^2 - MH, \quad (6)$$

128 where J is the magnetic exchange parameter between S_i and S_j nearest-neighbour spins, v volume and K
 129 compressibility.

130 All the parameters required to simulate a given (real) magnetic system using this approach can be readily
 131 obtained by existing DFT packages. Estimating J for multi-component alloys is particularly relevant in
 132 the study of magnetocaloric materials, so the use of the Liechtenstein method (Liechtenstein et al., 1987)
 133 in systems where fractional site occupancy is accurately described by the Coherent Potential Application
 134 (Yonezawa and Morigaki, 1973) is a practical approach. These capabilities are available in the SPR-
 135 KKR (H. Ebert et al.) and openmx (T. Ozaki et al.) DFT packages. The estimate of the full $M(H, T)$
 136 and $\Delta S_M(H, T)$ dependencies can be challenging using the standard Monte Carlo Metropolis method
 137 (Metropolis et al., 1953), as each (H, T) pair will require an independent calculation, and for the case of
 138 FOMPT the stabilization of the two order parameters, M and v is difficult and time-consuming. Another
 139 approach is to obtain the thermodynamic properties of the system with previously calculated Joint Density
 140 of States (JDOS) estimates. The JDOS of a given model (discrete or continuous) and of a given lattice (e. g.
 141 2D, 3D) can be calculated by Monte Carlo methods such as the Wang-Landau method (Wang and Landau,
 142 2001; Zhou et al., 2006), Random Path Sampling (Amaral et al., 2014) and the recently reported Flat Scan
 143 Sampling method (Inácio et al., 2022). As the JDOS is T , H and v independent, the full calculation of
 144 $M(H, T)$ and $\Delta S_M(H, T)$ dependencies for both SOMPT and FOMPT systems is robust and quickly
 145 achievable using a regular personal computer.

146 For describing a comparable system to the previous mean-field simulations, we consider the Ising model
 147 of 512 spin 1/2 particles in a 3D lattice. In the case of the rigid system with a SOMPT, the J value is
 148 chosen to lead to a T_C of 300 K. The field interaction is calculated with a magnetic moment value of 1
 149 μ_B per spin. Imposing a 100 emu/g saturation magnetization, a similar behavior compared to the previous
 150 mean-field models is obtained for magnetization and magnetic entropy change, as seen in Figure 5.

151 Considering now a compressible system, with a linear dependence of J on volume, $J(v) = J_0 + J'(v - v_0)/v_0$ and a K value of 50, a J' value of 2.8 (in units of J_0) leads to a FOMPT with a critical field of
 152 ~ 25 kOe, comparable to the previous simulations of the Landau Theory of phase transitions and the
 153 Bean-Rodbell model, as shown in Figure 6.

155 While qualitatively the behavior of the Ising model simulations for both SOMPT and FOMPT systems
 156 are similar to the results of the mean-field models, a quantitative comparison highlights some differences.

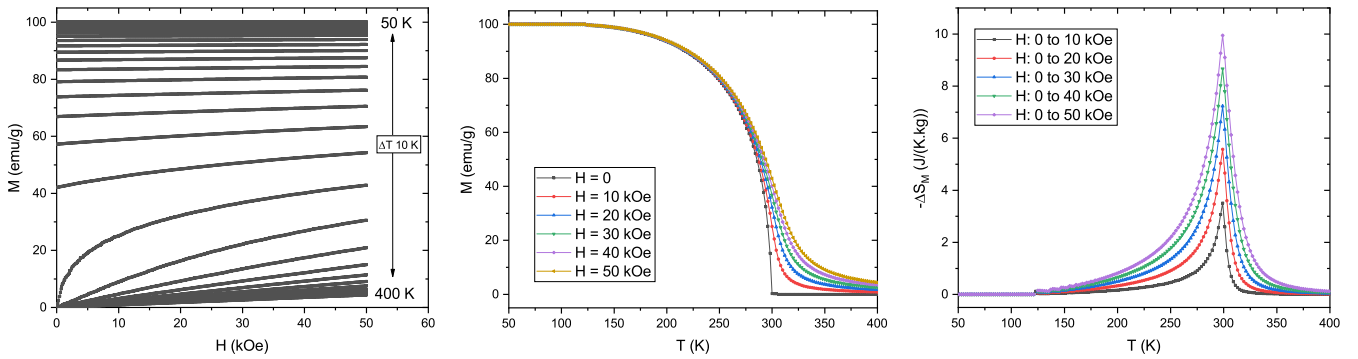


Figure 5. (A) Isothermal magnetization M versus applied magnetic field H , of a SOMPT system ($J' = 0$) from a Ising spin 1/2 3D lattice with 512 spins, considering a saturation magnetization of 100 emu/g and a magnetic moment value of $1 \mu_B$ per spin. (B) Isofield M versus temperature T behavior, for H between 0 and 50 kOe. (C) Magnetic entropy change ΔS_M dependence on H change and T .

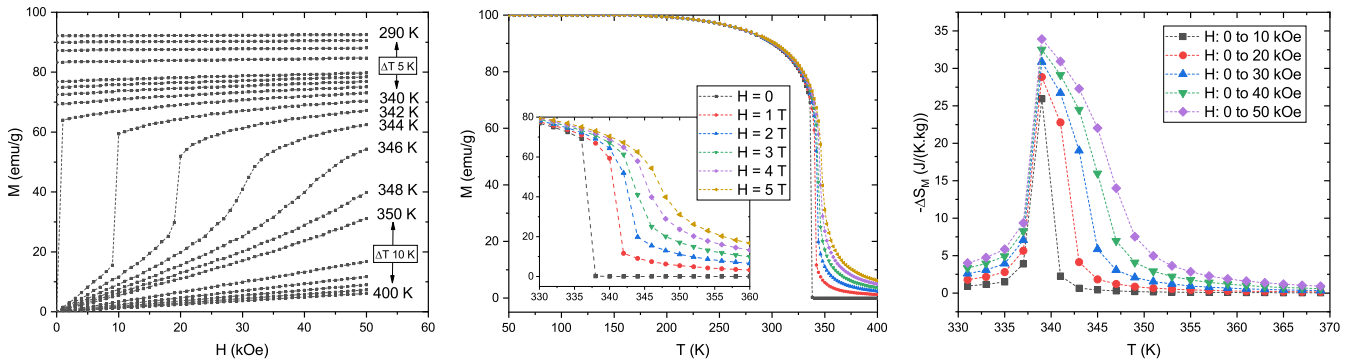


Figure 6. (A) Isothermal magnetization M versus applied magnetic field H , of a FOMPT system ($J' = 2.8$) from a compressible Ising spin 1/2 3D lattice with 512 spins, considering a saturation magnetization of 100 emu/g and a magnetic moment value of $1 \mu_B$ per spin. (B) Isofield M versus temperature T behavior, for H between 0 and 50 kOe. (C) Magnetic entropy change ΔS_M dependence on H change and T .

157 While for the mean-field models the change of T_C between the SOMPT and FOMPT is relatively small
 158 at around 3 K ($\sim 1\%$ of T_C), for the case of the microscopic model, this value is substantially higher
 159 at ~ 40 K ($\sim 13\%$ of T_C). In terms of the observed maximum values of $-\Delta S_M$ for an applied field
 160 of 50 kOe, for both SOMPT and FOMPT systems the obtained results are similar for all the considered
 161 models. These increase from ~ 10 J/(K·kg) of the SOMPT systems, to values ~ 35 J/(K·kg) for the FOMPT
 162 systems. These results highlight how these fundamentally different models can lead to quantitatively similar
 163 behaviors for both the $M(H, T)$ and $\Delta S_M(T, H)$ dependencies, with results comparable to real SOMPT
 164 and FOMPT materials.

5 OVERVIEW

165 In this work, we have explored three distinct magnetic models that can simulate the relevant thermodynamic
 166 properties of both SOMPT and FOMPT systems for application in magnetic refrigeration and thermal
 167 energy harvesting. One of the main objectives was to consider equivalent SOMPT and FOMPT magnetic

168 systems with T_C values around room temperature, and to compare the simulated results, particularly
169 $M(H, T)$ and $\Delta S_M(H, T)$, which are the main thermodynamic properties for these applications.

170 Landau theory allows to easily interpret experimental magnetization data by fitting the isothermal Arrott
171 plots. The observation of negative values of the B coefficient(negative slopes in the Arrott plots) is a sign
172 of a FOMPT. With a full description of the temperature dependence of the A , B and C coefficients, it is
173 straightforward to smooth, interpolate and, away for saturation, to extrapolate the (H, T) dependence of
174 magnetization and magnetic entropy change data. Still, while it is possible to qualitatively interpret the
175 values of the model parameters, they do not have a straightforward or quantitative physical interpretation.
176 Nevertheless, the obtained $M(H, T)$ and $\Delta S_M(H, T)$ data are physically and quantitatively sound.

177 The Bean-Rodbell model, as an extension of the Weiss molecular mean-field model, while also a
178 phenomenological model, has physical meaning to all its parameters. This allows to interpret experimental
179 data of both SOMPT and FOMPT systems and estimate fundamental system properties such as spin value
180 and quantify magnetovolume coupling. The validity of the simulations near M saturation, in contrast
181 to the Landau theory, allows for accurate description of GMCE systems in a wider temperature range,
182 including disordered and mixed phase systems. While the Bean-Rodbell simulation parameters have
183 physical meaning, it is impossible to directly obtain input values of T_O and β from ab-initio calculations
184 at 0 K. To allow the prediction of the properties of a given material from DFT calculations at 0K, then a
185 different approach is required.

186 A microscopic model approach, while typically more expensive in terms of computational cost, allows
187 for more intricate and detailed simulation of model systems. As the main simulation parameter J , together
188 with its dependence on system volume $J(v)$, are obtainable via DFT calculations, an in-silico approach
189 to predict the thermo-magnetic properties of new and optimized magnetic materials is possible. The
190 use of prior JDOS of models such as the Ising and Heisenberg models, lowers computational cost for
191 simulation of materials for arbitrary values of J and $J(v)$, and allows the description of the full $M(H, T)$
192 and $\Delta S_M(H, T)$ dependencies.

193 Our simulation results for the three models, for both SOMPT and FOMPT systems are both qualitatively
194 and quantitatively in agreement. The $M(H, T)$ and $\Delta S_M(H, T)$ behaviors are similar, particularly the
195 increase of the maximum ΔS_M value due to the change of a SOMPT to a FOMPT. The most notable
196 difference between our obtained results is the larger change of T_C of the FOMPT system compared to the
197 SOMPT, in the case of the compressible Ising model simulations. We highlight that all three models are
198 physically sound, and the choice of which one to use will depend if the purpose is to interpret experimental
199 data, or the in-silico prediction of the performance of new and optimized magnetic refrigerants and
200 ferromagnets for thermal energy harvesting.

CONFLICT OF INTEREST STATEMENT

201 The authors declare that the research was conducted in the absence of any commercial or financial
202 relationships that could be construed as a potential conflict of interest.

AUTHOR CONTRIBUTIONS

203 All authors contributed to conception and design of the study, contributed to manuscript revision, read, and
204 approved the submitted version.

FUNDING

205 This work was developed within the scope of the project CICECO-Aveiro Institute of Materials,
206 UIDB/50011/2020, UIDP/50011/2020 & LA/P/0006/2020, financed by national funds through the
207 FCT/MEC (PIDDAC).

REFERENCES

- 208 Gutfleisch O, Willard MA, Brück E, Chen CH, Sankar SG, Liu JP. Magnetic materials and devices for
209 the 21st century: Stronger, lighter, and more energy efficient. *Advanced Materials* **23** (2011) 821–842.
210 doi:<https://doi.org/10.1002/adma.201002180>.
- 211 Pecharsky VK, Gschneidner Jr KA. Giant magnetocaloric effect in $\text{Gd}_5(\text{Si}_2\text{Ge}_2)$. *Phys. Rev. Lett.* **78** (1997)
212 4494–4497. doi:<https://doi.org/10.1103/PhysRevLett.78.4494>.
- 213 Pecharsky VK, Gschneidner Jr KA. Thirty years of near room temperature magnetic cooling: Where we
214 are today and future prospects. *Int. J. Refrig.* **31** (2008) 945–961. doi:<https://doi.org/10.1016/j.ijrefrig.2008.01.004>.
- 216 Kitanovski A, Tušek J, Tomc U, Plazník U, Ožbolt M, Poredoš A. *Magnetocaloric Energy Conversion - From Theory to Applications* (Springer) (2015).
- 218 Waske A, Dzekan D, Sellschopp K, Berger D, Stork A, Nielsch K, et al. Energy harvesting near room
219 temperature using a thermomagnetic generator with a pretzel-like magnetic flux topology. *Nature Energy*
220 **4** (2019) 68–74. doi:<https://doi.org/10.1038/s41560-018-0306-x>.
- 221 Amaral VS, Amaral JS. Magnetoelastic coupling influence on the magnetocaloric effect in ferromagnetic
222 materials. *J. Magn. Magn. Mat.* **272-276** (2004) 2104–2105. doi:<https://doi.org/10.1016/j.jmmm.2003.12.870>.
- 224 Amaral JS, Amaral VS. The effect of magnetic irreversibility on estimating the magnetocaloric effect
225 from magnetization measurements. *Appl. Phys. Lett.* **94** (2009) 042506. doi:<https://doi.org/10.1063/1.3075851>.
- 227 Amaral JS, Reis MS, Amaral VS, Mendonça TM, Araújo JP, Sá MA, et al. Magnetocaloric effect in Er-
228 and Eu-substituted ferromagnetic La-Sr manganites. *J. Magn. Magn. Mat.* **290-291** (2005) 686–689.
229 doi:<https://doi.org/10.1016/j.jmmm.2004.11.337>.
- 230 Bean CP, Rodbell DS. Magnetic disorder as a first-order phase transformation. *Phys. Rev.* **126** (1962)
231 104–114. doi:<https://doi.org/10.1103/PhysRev.126.104>.
- 232 Amaral JS, Amaral VS. On estimating the magnetocaloric effect from magnetization measurements. *J.*
233 *Magn. Magn. Mat.* **322** (2010) 1552–1557. doi:<https://doi.org/10.1016/j.jmmm.2009.06.013>.
- 234 Amaral JS, Silva NJO, Amaral VS. A mean-field scaling method for first- and second-order phase
235 transition ferromagnets and its application in magnetocaloric studies. *Appl. Phys. Lett.* **91** (2007) 172503.
236 doi:<https://doi.org/10.1063/1.2801692>.
- 237 Amaral JS, Tavares PB, Reis MS, Araújo JP, Mendonça TM, Amaral VS, et al. The effect of chemical
238 distribution on the magnetocaloric effect: A case study in second-order phase transition manganites. *J.*
239 *Non-cryst. Sol.* **354** (2008) 5301–5303. doi:<https://doi.org/10.1016/j.jnoncrysol.2008.05.078>.
- 240 Bahl CRH, Bjørk R, Smith A, Nielsen KK. Properties of magnetocaloric materials with a distribution of
241 curie temperatures. *J. Magn. Magn. Mat.* **324** (2012) 564–568. doi:<https://doi.org/10.1016/j.jmmm.2011.08.044>.
- 243 Amaral JS, Amaral VS. Disorder effects in giant magnetocaloric materials. *Phys. Stat. Sol. A* **211** (2014)
244 971–974. doi:<https://doi.org/10.1002/pssa.201300749>.

- 245 Nielsen KK, Bahl CRH, Smith A, Bjørk R. Spatially resolved modelling of inhomogeneous materials
246 with a first order magnetic phase transition. *J. Phys. D: Appl. Phys.* **50** (2017) 414002. doi:<https://doi.org/10.1088/1361-6463/aa86e2>.
- 248 Amaral JS, Fortunato NM, Amorim CO, Gonçalves JN, Amaral VS. Giant magnetocaloric effect of
249 compressible ising and heisenberg lattices. *Proceedings of the 7th International Conference on Magnetic*
250 *Refrigeration at Room Temperature (Thermag VII)* (2016) 30019341. doi:<http://dx.doi.org/10.18462/iir.thermag.2016.0200>.
- 252 Liechtenstein AI, Katsnelson MI, Antropov VP, Gubanov VA. Local spin density functional approach to
253 the theory of exchange interactions in ferromagnetic metals and alloys. *J. Magn. Magn. Mat.* **67** (1987)
254 65–74.
- 255 Yonezawa F, Morigaki K. Coherent potential approximation. basic concepts and applications. *Progress of*
256 *Theoretical Physics Supplement* **53** (1973) 1–76. doi:<https://doi.org/10.1143/PTPS.53.1>.
- 257 [Dataset] H Ebert et al. The Munich SPR-KKR package (????).
- 258 [Dataset] T Ozaki et al. Openmx (open source package for material explorer) (????).
- 259 Metropolis N, Rosenbluth AW, Rosenbluth MN, Teller AH, Teller E. Equation of state calculations by fast
260 computing machines. *J. Chem. Phys.* **21** (1953) 1087.
- 261 Wang F, Landau DP. Efficient, multiple-range random walk algorithm to calculate the density of states.
262 *Phys. Rev. Lett* **86** (2001) 2050.
- 263 Zhou STC, Schultheiss TC, Landau DP. Wang-Landau algorithm for continuous models and joint density
264 of states. *Phys. Rev. Lett.* **96** (2006) 120201.
- 265 Amaral JS, Gonçalves JN, Amaral VS. Thermodynamics of the 2-D ising model from a random path
266 sampling method. *IEEE Trans. Magn.* **50** (2014) 1002204.
- 267 Inácio JC, Ferreira AL, Amaral JS. Accurate estimate of the joint density of states via flat scan sampling.
268 *arXiv arXiv:2203.02718* (2022). doi:<https://doi.org/10.48550/arXiv.2203.02718>.